Journal of
Instrumentation

Investigation of dielectronic recombination in neon ions using EBIT

Published by IOP Publishing for Sissa Medialab

Received: *January 7, 2025*
Accepted: *March 28, 2025*
Published: *April 29, 2025*

The 15th International Symposium on Electron Beam Ion Sources and Traps
Kielce, Poland
27–30 August 2024

Investigation of dielectronic recombination in neon ions using EBIT

W. Biela-Nowaczyk,[a,b,c,*] **D. Banaś**,[a] **F. Grilo**,[d] **Ł. Jabłoński**,[a] **R. Stachura**[a] **and A. Warczak**[c]

[a] *Institute of Physics, Jan Kochanowski University, Uniwersytecka 7, 25-406 Kielce, Poland*
[b] *GSI Helmholtzzentrum für Schwerionenforschung GmbH, Planckstraße 1, 64291 Darmstadt, Germany*
[c] *Institute of Physics, Jagiellonian University, Łojasiewicza 11, 30-348 Cracow, Poland*
[d] *Laboratory of Instrumentation, Biomedical Engineering and Radiation Physics (LIBPhys-UNL), NOVA School of Science and Technology, NOVA University Lisbon, Physics Campus da Caparica, 2829-516 Caparica, Portugal*

E-mail: weronika.biela-nowaczyk@ujk.edu.pl

Abstract: Electron Beam Ion Traps (EBITs) provide a controlled environment for studying electron-ion interactions, particularly in highly charged ions (HCIs), and enable precise measurement of processes, such as dielectronic recombination (DR). Using the compact Dresden EBIT at Jagiellonian University, we present new experimental data on DR in neon ions, collected for electron energy scanned in range of 700 to 1000 eV. The data were obtained with a silicon-drift X-ray detector (Bruker XFlash 5030), and results indicate resonant structures corresponding to DR, with the observed resonant-like K_β emission primarily attributed to He-like neon ions. However, low statistical precision highlights the challenges of achieving optimal signal quality in this setup, particularly due to low detection efficiency in the K-shell neon energy range. Planned improvements, including repositioning the detector closer to the trap and removing the beryllium window, are expected to enhance resolution and data acquisition efficiency in future studies.

Keywords: Ion sources (positive ions, negative ions, electron cyclotron resonance (ECR), electron beam (EBIS)); Data analysis

*Corresponding author.

https://doi.org/10.1088/1748-0221/20/04/C04034

2025 JINST 20 C04034

Contents

1 Introduction 1

2 Methodology and experimental design 2

3 Theoretical modeling and computational approach 4

4 Experimental observation of dielectronic recombination in neon 5

5 Conclusions 7

1 Introduction

For decades, Electron Beam Ion Traps (EBITs) have played a significant role in advancing our understanding of electron-ion collision processes, providing essential data that bridges laboratory experiments and astrophysical phenomena. EBITs are uniquely suited for producing and trapping highly charged ions (HCIs), enabling precise measurements of important processes such as dielectronic recombination (DR). These contributions are critical in studying astrophysical plasmas and interpreting X-ray emissions from cosmic sources [1].

Dielectronic recombination (DR) is a two-step resonant process that occurs only when the precise resonance condition for an ion-electron collision is met. In the first step, known as dielectronic capture, which is the time-reversed of the Auger process, a free electron is captured by an ion with simultaneous excitation of an inner electron to a higher atomic shell. This highly specific energy condition is what makes DR a resonant process: the energy gained during this capture must precisely match the amount required to simultaneously excite an inner electron. Previously, we reported experimental results on DR for argon and cerium ions [2–4]. Following dielectronic capture, the system can proceed via radiative de-excitation, resulting in the emission of characteristic X-rays and this two step process is called DR. Alternatively, it may undergo de-excitation through the Auger effect, where the energy is released by ejecting an electron. As a result, understanding dielectronic recombination (DR) requires consideration of competing pathways like Auger decay, which can reduce the probability of radiative emission. DR plays a crucial role in the cooling of astrophysical plasmas [5] and in shaping the ionization balance of these environments, making them essential for understanding the evolution of stellar and galactic systems. Importantly, DR can be directly observed by cosmic telescopes [6], underscoring the significance of its investigation in laboratory settings.

The astrophysical importance of DR is underscored by large-scale missions such as Chandra [7], XMM-Newton [8], Hitomi [9], Athena [10], and recently, XRISM [11]. These missions aim to decode X-ray emissions from cosmic sources such as galaxy clusters and supernova remnants, many of which exhibit signatures from highly charged ions. Accurate laboratory data is therefore crucial for interpreting the X-ray spectra observed by these missions.

Neon, one of the most abundant elements in the Universe, holds particular relevance in these studies due to its presence in various astrophysical plasmas. Previous investigations into the DR of neon ions using ion storage rings focused on Ne^{5+} [12, 13] and Ne^{3+} [14]. However, no comprehensive

2025 JINST 20 C04034

EBIT data for neon has been published until now. While the present work provides new insights into neon's DR, the poor statistical quality of the data highlights the challenges of studying this system using the EBIT setup. Further research is needed to fully investigate the electron-ion interactions of neon, particularly in the context of astrophysical plasmas.

2 Methodology and experimental design

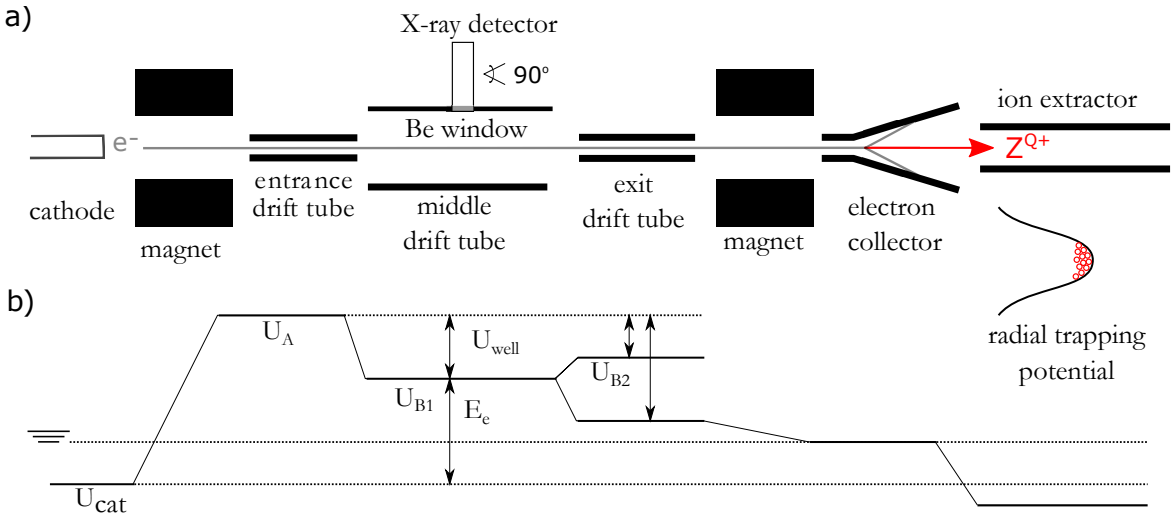

Figure 1. (a) Schematic of the Model S EBIT (DREEBIT). (b) Representation of all voltages at each electron beam stage.

A compact, room-temperature EBIT [15, 16] system was utilized for this experiment at Jagiellonian University (UJ). The UJ-EBIT, produced by DREEBIT, is designed for ion trapping and electron-ion collision studies. Equipped with an X-ray detector (Bruker XFlash 5030), the facility enables comprehensive investigations into radiative processes. The schematic of the trap is shown in figure 1. The electron beam is generated by a heated cathode (0.5 mm in diameter) under a negative bias, then accelerated by potential difference of cathode and electrodes inside the EBIT ($U_{cat} + U_A$, figure 1). Moreover, the electron beam is confined radially by permanent magnets with a magnetic induction of 250 mT, reducing the beam radius to about 25 µm [17, 18]. The pressure inside the trap was maintained at 10^{-10} mbar before introducing a controlled flow of high-purity neon gas. The electron beam traverses the neon gas, ionizing the atoms and producing Ne ions of various charge states.

Ion trapping within the EBIT is achieved axially by a series of positively biased cylindrical drift tubes (U_A, U_{B1} and U_{B2} — shaping the potential well, shown in figure 1), while radial ion trapping is maintained by the space charge of the electron beam (figure 1) enhanced by the applied magnetic field. The magnetic field plays a crucial role in this process, as it not only defines the spatial size of the electron beam but also influences the charge state distribution of the trapped ions. In EBITs with a strong magnetic field (e.g., FLASH-EBIT [19]), higher beam currents can enhance ionization efficiency, often leading to a charge state distribution concentrated around a single charge state. However, in our apparatus, we typically observe a broader charge state distribution, with multiple charge states coexisting within the EBIT plasma [20]. This broader distribution can be attributed to the residual pressure within the system, where the charge exchange with neutral particles is competing with

2025 JINST 20 C04034

the ionization process. The variability in charge states within our EBIT is particularly significant when discussing resonant processes such as dielectronic recombination (DR). One key consideration is the energy spread of electrons within the EBIT, which affects the precision of the resonance condition. In planning our experiments, we typically assume that ion distribution is stable and that the ion-electron collision energy is well-defined, based on the difference in voltages between the cathode and the middle drift tube ($E_e = U_C + U_A - U_{B1}$, figure 1) with a correction for the space charge potential. However, both ions and electrons possess a distribution of energies, which introduces a spread in the actual collision energies. As a result, the resonance condition for DR is met not at a single, precise energy, but within a specific energy range around the set ion-electron collision energy. It is often used to assume value of 30 eV energy spread, eg. while making a simulations of DR.

For X-ray detection, a silicon-drift detector (XFlash Bruker 5030) was positioned perpendicular to the electron beam axis at the center of the trap. The detector has an energy resolution of ~127 eV (FWHM) at the Mn K_α line, has an active area of 30 mm^2 and 12.5 µm thick Be window. Combined with the second 12.5 µm Be window of the EBIT chamber (effective 25 µm thickness) the setup provides approximately 97% detection efficiency for Ar K-shell X-rays, therefore Ar has been intensively studied before. However, the detection on Ne K-shell X-ray is at the level of few percent (see figure 2).

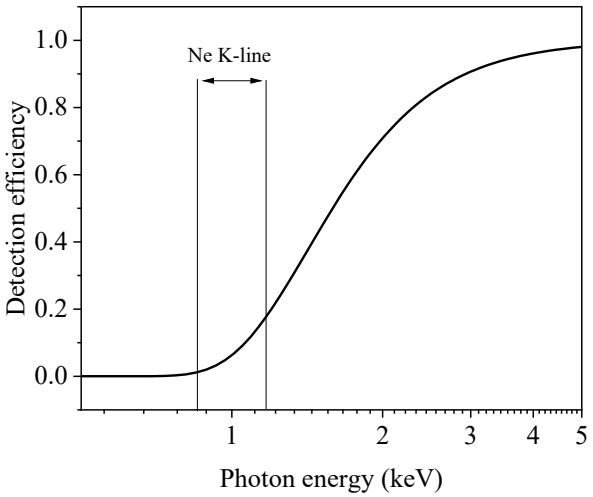

Figure 2. The detection efficiency of XFlash Bruker 5030 for two different thickness of beryllium window.

Data acquisition was performed using the TERX Detection System, which offers a scanning procedure of electron energy over a given range. In most EBIT experiments, a fast scanning procedure is employed, where the voltage setting of the middle drift tube is changed across the entire range of interest within eg. 80 ms of measurement [21]. After this scan, the ions are extracted, and the measurement is repeated. This fast scan method is advantageous because it allows the investigation of the entire energy range while maintaining the same charge state distribution. As a result, the well-established theoretical and experimental cross section of radiative recombination (RR) can be used as a reference to estimate the cross section for the process of interest, like dielectronic recombination (DR). In our experiment, however, we implemented a different approach: we measured the selected electron energy range for 500 ms, then released the ions, adjusted the voltages, and repeated the measurement. This slower scanning process does not allow for a direct comparison of cross sections, as the charge state distribution may vary between measurement steps. We opted for a slower scanning approach to achieve a more stable charge state distribution at each electron energy setting and improve the clarity of weak spectral features. While a fast scan can accumulate equivalent total measurement time across the energy range, the rapid cycling introduces variations in ion charge states, potentially masking subtle signals. By holding each energy setting constant for an extended period, the slow scan reduces these fluctuations, allowing for clearer identification of weak processes and subtle spectral features that might be overlooked in a fast scan.

2025 JINST 20 C04034

3 Theoretical modeling and computational approach

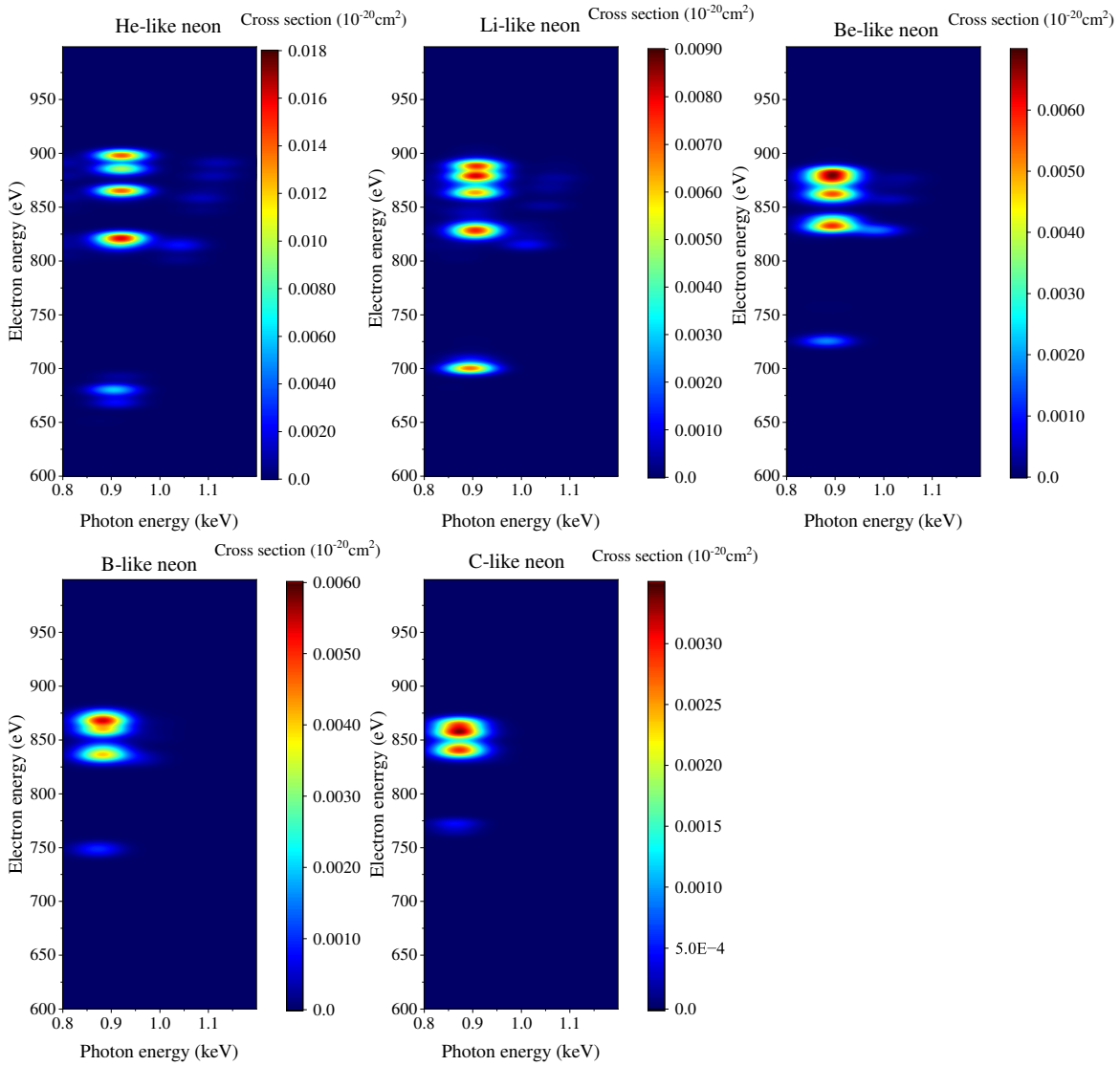

Figure 3. Results of FAC calculations of DR KLn for n = 2, 3, 4, 5, 6 for various charge states of neon.

To develop theoretical models for the processes of interest, we employed the Flexible Atomic Code (FAC) [22]. FAC is a comprehensive software package designed for calculating a broad range of atomic radiative and collisional processes. It accurately computes energy levels, radiative transition rates, collisional excitation and ionization rates, as well as more complex phenomena such as photoionization, radiative recombination, autoionization, and dielectronic capture. For this study, FAC's collisional radiative model was particularly valuable, as it allowed us to generate synthetic spectra for dielectronic recombination in specific ion charge states. The results of FAC calculations for neon ions are shown in figure 3. The raw FAC results are discrete resonances, pinpointing electron energies that satisfy the resonance conditions and identifying the photon energies associated with radiative relaxation pathways. To better visualize the modeled spectrum in three dimensions, we applied additional broadening: 80 eV for photon energy (based on [23]) and 8 eV for electron energy broadening.

2025 JINST 20 C04034

Here, we draw the reader's attention to the fact that only in the cases of He-like, Li-like, and Be-like neon ions the K_β transition is observed as a de-excitation channel. For ions with lower charge states, only the K_α transition occurs, due to differences in radiative rates for various radiative pathways of selected ion states. Figure 4 shows a projection of the theoretically calculated K_β radiation onto the electron energy axis (presented in figure 3), illustrating the resonant energies where the K_β de-excitation is produced for dielectronic recombination processes in neon.

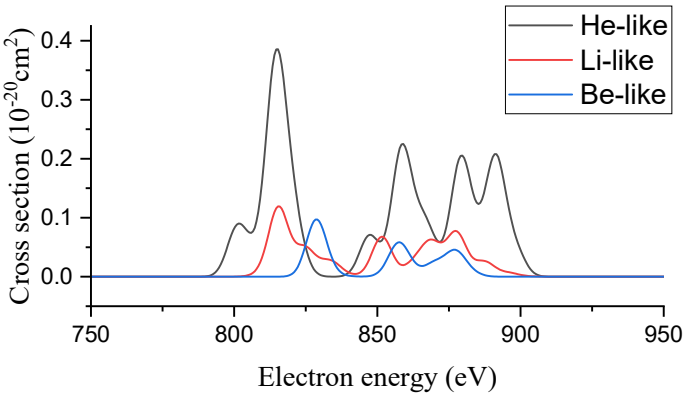

Figure 4. The projection of cross section of DR in neon resulting with a K_β radiation as a function of electron energy.

4 Experimental observation of dielectronic recombination in neon

We conducted data collection for dielectronic recombination (DR) in neon ions across two experimental runs. In the first run, we scanned a broad electron energy range from 600 to 1450 eV in 2 eV steps, maintaining a neon gas pressure level of 1.4×10^{-9} mbar. The resulting experimental data are shown in figure 5(a). From this experiment, we observed significantly lower detection efficiency for K_α transitions compared to K_β transitions. The spectrum reveals only isolated counts indicating the K_α line location, while the K_β line appears as a distinct vertical line slightly above 1 keV. Additionally, we observed clear radiative recombination (RR) lines associated with the K and L shells. The RR line for the K shell corresponds to recombination to Ne^{9+} ions, while RR to Ne^{10+} ions was not registered here, as the electron energy range was too low to produce bare ions effectively. Notably, figure 5(a) displays an enhanced count rate at the intersection of the extended K_β line and the L-shell RR line, a location characteristic of DR K-LM processes, highlighted with a red ellipse.

In the second experimental run, we focused on the specific spectral region depicted in figure 5(a), scanning the electron energy range from 700 to 1000 eV in steps of 1 eV and increasing the gas pressure to 3×10^{-9} mbar. The resulting spectrum is shown in figure 5(b). Gathering data over this selected 300 eV energy range took more than 100 hours. Despite the extended measurement time the data statistics remain relatively low, however, three clusters of counts can be observed at three or four selected electron energies where the resonance condition is met. To better visualize these structures, data from both collections were combined and projected onto the electron energy axis, as displayed in figure 6(a). It is important to remember that, based on the energy of the detected radiation, these features have been identified as K_β radiation. In the electron energy projection, an increase in registered counts can be observed around electron energies of approximately 813 eV, 858 eV, and 878 eV, with a broader structure around 895 eV. The calibration of these data was adjusted by an additional 4 eV factor, following previous calibration including space charge potential correction.

2025 JINST 20 C04034

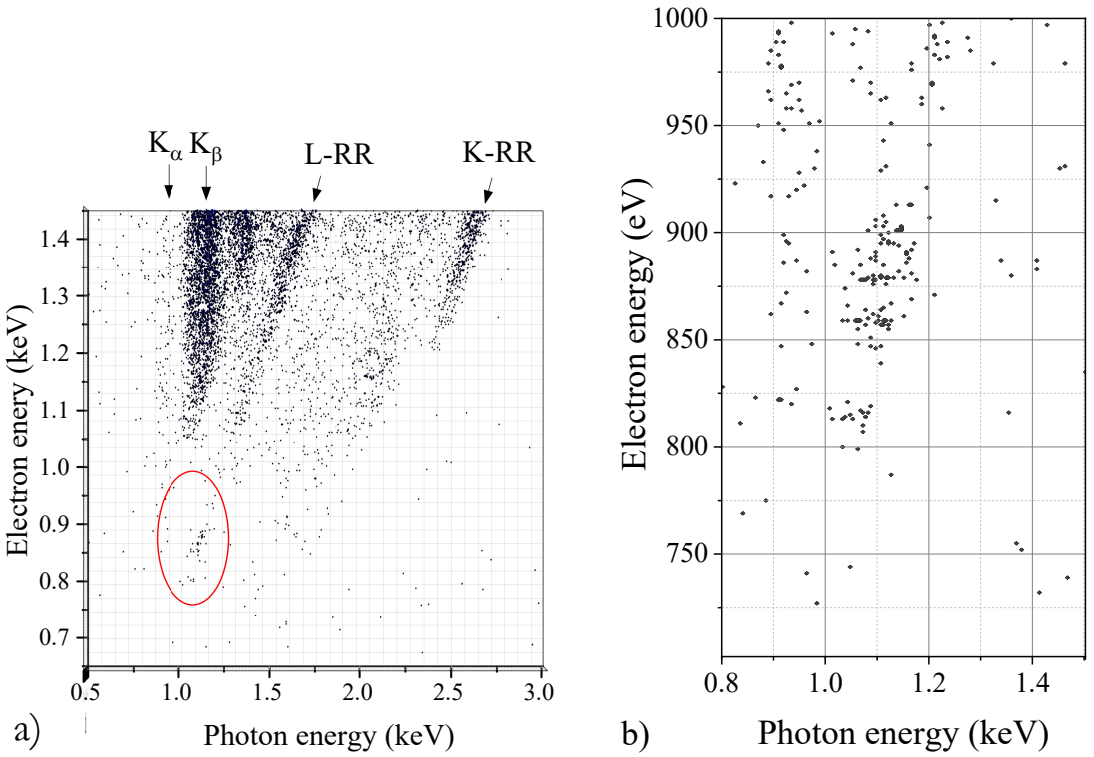

Figure 5. (a) Spectrum of K_β radiation, radiative recombination (RR) and dielectronic recombination (DR, red elipse) in neon ions, measured over a broad electron energy range from 600 to 1450 eV with a neon gas pressure of 1.4×10^{-9} mbar. (b) Spectrum focused on the DR K-LM region identified in (a), with electron energies from 700 to 1000 eV and an increased gas pressure of 3×10^{-9} mbar. This higher-resolution scan allows for closer examination of the features in the selected energy region.

The measured values can be compared with the calculated resonant energies (previously shown in figure 4), as presented in figure 6. Panel (a) shows the projection of the experimental data onto the electron energy axis, while panel (b) displays the results of the FAC calculations. It is important to note that the experimental data have been shifted by 4 eV for alignment, and within this adjustment, the agreement with theory is evident. The figures clearly demonstrate that the measured structures correspond to the calculated ones. Based on the figure 4(b) one can see that for He-like neon ions, the resonance condition is met at 814.5 eV, 858.5 eV, and 878.5 eV, with a group of resonances near 890 eV. For Li-like neon ions, resonance occurs at 815.5 eV, 851.5 eV, and 877.5 eV, whereas for Be-like ions, the resonance condition is fulfilled at 857.5 eV and 877.5 eV. Given the current statistics, we cannot draw conclusions about the charge state distribution of neon ions. However, since He-like ions are more likely to produce K_β radiation compared to other charge states (the DR resonant strength shown in figure 6(b), it appears that in this case, we have observed dielectronic recombination predominantly in He-like neon ions. Still, this doesn't allow to draw the conclusions about the neon charge state distribution inside the EBIT. Further studies with improved statistics and extended measurement times would be necessary to gain more detailed insights into the ion distribution and the role of various charge states in the observed processes.

2025 JINST 20 C04034

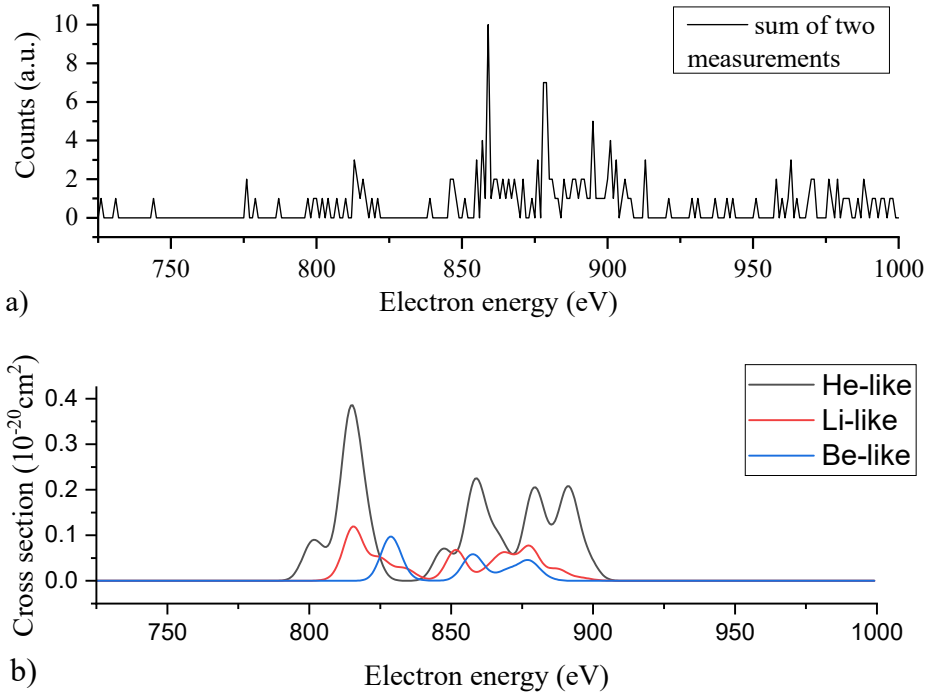

Figure 6. (a) Projection of experimental data onto the electron energy axis, highlighting resonant electron energies where increased count rates are observed at approximately 813 eV, 858 eV, 878 eV, and a broadened feature near 895 eV. Calibration includes additional 4 eV correction. (b) Calculation results as presented in figure 4 for comparisson purposes.

5 Conclusions

In conclusion, this study presents new insights into the electron-ion interactions of neon, specifically targeting a spectral range previously lacking data, as noted in the introduction in reference to the astrophysical experiments. Despite the progress made, the limited statistics in this experiment underscore the challenges of studying neon interactions with the current EBIT setup. This highlights the need for further investigations to enhance our understanding of neon's resonant structures and charge states in EBIT. To address these limitations, future experiments are planned to be conducted with a detector positioned closer to the trap and without the beryllium window, which will significantly improve data acquisition efficiency and spectral resolution.

Acknowledgments

D. Banaś, Ł. Jabłoński, R. Stachura and W. Biela-Nowaczyk are grateful for the financial support by the Minister of Science (Poland) under the "Regional Excellence Initiative" program (project no.: RID/SP/0015/2024/01).

2025 JINST 20 C04034

References

[1] P. Beiersdorfer, *Laboratory x-ray astrophysics*, *Ann. Rev. Astron. Astrophys.* **41** (2003) 343.

[2] W. Biela, A. Warczak, A. Mucha and A. Malarz, *Enhanced Ar-K X-ray emission observed in EBIT at electron energies around 6,500 eV*, *X Ray Spectrom.* **48** (2019) 696.

[3] W. Biela-Nowaczyk, P. Amaro, F. Grilo and A. Warczak, *Higher-Order Recombination Processes in Argon Ions Observed via X-ray Emission in an EBIT*, *Atoms* **11** (2022) 1.

[4] W. Biela-Nowaczyk, F. Grilo, P. Amaro and A. Warczak, *L-Mn dielectronic recombination of cerium ions in a room-temperature EBIT*, *J. Phys. B* **57** (2024) 055201.

[5] J. Dubau and S. Volonte, *Dielectronic recombination and its applications in astronomy*, *Rept. Prog. Phys.* **43** (1980) 199.

[6] A.H. Gabriel, *Dielectronic Satellite Spectra for Highly-Charged Helium-Like Ion Lines*, *Mon. Not. Roy. Astron. Soc.* **160** (1972) 99.

[7] M.C. Weisskopf, H.D. Tananbaum, L.P. van Speybroeck and S.L. O'Dell, *Chandra x-ray observatory (cxo):overview*, *Proc. SPIE* **4012** (2000) 2 [astro-ph/0004127].

[8] F. Jansen et al., *XMM-Newton observatory. I. The spacecraft and operations*, *Astron. Astrophys.* **365** (2001) L1.

[9] T. Takahashi et al., *The ASTRO-H (Hitomi) x-ray astronomy satellite*, *Proc. SPIE* **9905** (2016) 212.

[10] X. Barcons et al., *Athena: the X-ray observatory to study the hot and energetic Universe*, *J. Phys. Conf. Ser.* **610** (2015) 012008.

[11] M.S. Tashiro et al., *Status of x-ray imaging and spectroscopy mission (XRISM)*, in the proceedings of the *Space Telescopes and Instrumentation 2020: Ultraviolet to Gamma Ray*, *Proc. SPIE* **11444** (2020) 293.

[12] S. Ali et al., *Experimental recombination rate coefficients of B-like carbon and B-like neon*, *Phys. Scripta T* **156** (2013) 014049.

[13] S. Mahmood et al., *Recombination rate coefficients of boron-like Ne*, *Astrophys. J.* **771** (2013) 78.

[14] E.B. Menz, *Preparation and Realisation of first Dielectronic Recombination Experiments at CRYRING@ESR*, Ph.D. Thesis, Friedrich Schiller University Jena, Jena, Germany (2024) [DOI:10.22032/dbt.64496].

[15] G. Zschornack et al., *Compact electron beam ion sources/traps: Review and prospects (invited)*, *Rev. Sci. Instrum.* **79** (2008) 02A703.

[16] G. Zschornacka, M. Schmidt and A. Thorn, *Electron Beam Ion Sources*, in the proceedings of the *CAS — CERN Accelerator School: Ion Sources*, Senec, Slovakia, 29 May–8 June 2012 [DOI:10.5170/CERN-2013-007.165] [arXiv:1410.8014].

[17] G. Herrmann, *Optical Theory of Thermal Velocity Effects in Cylindrical Electron Beams*, *J. Appl. Phys.* **29** (1958) 127.

[18] F. Currell and G. Fussmann, *Physics of electron beam ion traps and sources*, *IEEE Trans. Plasma Sci.* **33** (2005) 1763.

[19] C. Shah et al., *Revisiting the Fe XVII line emission problem: laboratory measurements of the 3s-2p and 3d-2p line-formation channels*, *Astrophys. J.* **881** (2019) 100 [arXiv:1903.04506].

[20] W. Biela, A. Warczak, A. Mucha and A. Malarz, *Charge State Evolution in Electron Beam Ion Trap*, *Acta Phys. Polon. B* **13** (2020) 975.

[21] F. Grilo et al., *Comprehensive Laboratory Measurements Resolving the LMM Dielectronic Recombination Satellite Lines in Ne-like Fe XVII Ions*, *Astrophys. J.* **913** (2021) 140 [arXiv:2106.04746].

[22] M.F. Gu, *The flexible atomic code*, *Can. J. Phys.* **86** (2008) 675.

[23] Ł Jabłoński et al., *Experimental investigations of two-electron relaxation processes in Rydberg hollow atoms*, *X Ray Spectrom.* **52** (2023) 430.

2025 JINST 20 C04034